journal of prosthodontic research 62 (2018) 24–30

Contents lists available at ScienceDirect

Journal of Prosthodontic Research

journal homepage: www.elsevier.com/locate/jpor

Original article

In vitro fatigue tests and *in silico* finite element analysis of dental implants with different fixture/abutment joint types using computer-aided design models

Satoshi Yamaguchi[a,*], Yasufumi Yamanishi[b], Lucas S. Machado[c], Shuji Matsumoto[a], Nick Tovar[c], Paulo G. Coelho[c], Van P. Thompson[d], Satoshi Imazato[a]

[a] Department of Biomaterials Science, Osaka University Graduate School of Dentistry, 1-8 Yamadaoka, Suita, Osaka 565-0871, Japan
[b] Department of Fixed Prosthodontics, Osaka University Graduate School of Dentistry, 1-8 Yamadaoka, Suita, Osaka 565-0871, Japan
[c] Department of Biomaterials and Biomimetics, New York University College of Dentistry,345 E 24th Street, New York, NY 10010, USA
[d] Department of Biomaterials and Biophotonics, Kings College London Dental Institute, Guy's Hospital, London, UK

ARTICLE INFO

Article history:
Received 27 October 2016
Received in revised form 10 March 2017
Accepted 28 March 2017
Available online 17 April 2017

Keywords:
Bioengineering
Finite element analysis
Fatigue test
Dental implant-abutment design
Step-stress accelerated life tests

ABSTRACT

Purpose: The aim of this study was to evaluate fatigue resistance of dental fixtures with two different fixture-abutment connections by *in vitro* fatigue testing and *in silico* three-dimensional finite element analysis (3D FEA) using original computer-aided design (CAD) models.
Methods: Dental implant fixtures with external connection (EX) or internal connection (IN) abutments were fabricated from original CAD models using grade IV titanium and step-stress accelerated life testing was performed. Fatigue cycles and loads were assessed by Weibull analysis, and fatigue cracking was observed by micro-computed tomography and a stereomicroscope with high dynamic range software. Using the same CAD models, displacement vectors of implant components were also analyzed by 3D FEA. Angles of the fractured line occurring at fixture platforms *in vitro* and of displacement vectors corresponding to the fractured line *in silico* were compared by two-way ANOVA.
Results: Fatigue testing showed significantly greater reliability for IN than EX ($p < 0.001$). Fatigue crack initiation was primarily observed at implant fixture platforms. FEA demonstrated that crack lines of both implant systems *in vitro* were observed in the same direction as displacement vectors of the implant fixtures *in silico*.
Conclusions: In silico displacement vectors in the implant fixture are insightful for geometric development of dental implants to reduce complex interactions leading to fatigue failure.

1. Introduction

Marginal bone loss of dental implants occurs regardless of preventive measures [1] and despite the high success rates of dental implant therapy [2–5]. Marginal bone loss may be caused by surgical trauma [6], excessive occlusal loading [7], microbial contamination of the implant fixture-abutment microgap [8], fixture-abutment micromovement [9], and repeated screwing and unscrewing [10]. While a substantial amount of research has focused on these topics over the past three decades, a breakthrough engineering design that reduces these complex interactions leading to failure has yet to be elucidated.

To investigate the influence of mechanical stress/strain on the marginal bone of dental implants, the design of implant components has been explored. Internal joint types have been established as fixture-abutment joint types with greater fatigue resistance [11–13] and stability [14] and lower degrees of microgap [15] and bone loss [16,17] relative to conventional external joint types.

While positive results relative to external hexagon platforms have been reported, internal connection designs may present substantial design parameter variations that include the shape of the abutment, presence or absence of platform switching, and the shape of the implant fixture neck. Consequently, a clear reason for the mechanical stress/strain concentration of the marginal bone

* Corresponding author. Fax: +81 6 6879 2919.
E-mail address: yamagu@dent.osaka-u.ac.jp (S. Yamaguchi).

http://dx.doi.org/10.1016/j.jpor.2017.03.006
1883-1958/

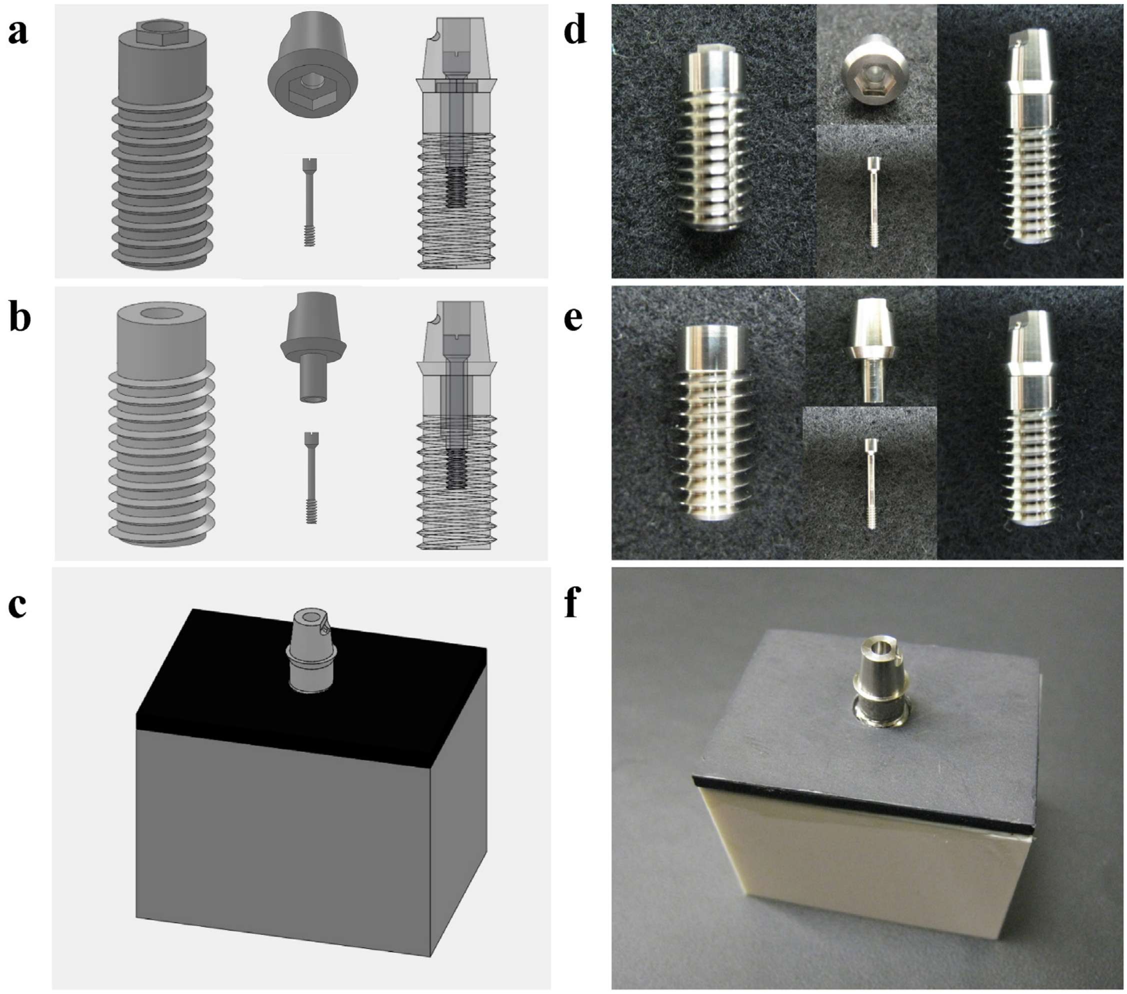

Fig. 1. Original CAD models and fabricated specimens. (a) CAD models of implant components (implant fixture, abutment, and abutment screw) and assembly with EX. (b) CAD models of implant components (implant fixture, abutment, and abutment screw) and assembly with IN. (c) Assembled model for 3D FEA. (d) Fabricated implant components from CAD models with EX and assembly. (e) Fabricated implant components from CAD models with IN and assembly. (f) Specimen for SSALTs.

has not been clarified, warranting optimization of multifactorial designs of implant components [18].

In vitro fatigue tests are one of the evaluation methods used to investigate the clinical reliability of dental implants. However, *in vitro* fatigue tests may fail to pinpoint the crack initiation site, even with the use of imaging techniques such as micro-computed tomography (micro-CT) or fractographic analysis. Therefore, step-stress accelerated life tests (SSALTs), which mimic mouth motion sliding contact, have been used to investigate the reliability of dental implants [19].

With this in perspective, *in silico* finite element analysis (FEA) is a useful approach to make comparisons focused on mono-factorial design [20] as it allows visualization and quantification of mechanical stress/strain distribution of the marginal bone of dental implant fixtures and implant components. Our previous work suggested that internal joint types are biomechanically more suitable than external joint types by using original computer-aided design (CAD) models [21]. Such results have been further supported by a number of *in silico* FEA studies using commercial dental implants containing mixed independent variables [12,22–24].

In this study, fatigue resistance of dental implants with two different implant/abutment joint types, the internal joint type and the external joint type, were evaluated by *in vitro* SSALT and *in silico* FEA employing our original CAD models. In addition, fatigue crack lines of the implant fixture *in vitro* and corresponding *in silico* displacement vectors were investigated.

2. Material and methods

2.1. Sample preparation

Dental implants with an external joint (EX) or an internal joint (IN) were machined from original CAD models (Fig. 1a–c) using ASTM grade IV titanium (GC Corp. Tokyo, Japan). The diameter and length (from the platform to the tip) of the implant fixture measured 5 × 13 mm, and the pitch of the threads measured 0.9 mm. The shape of the threads and abutment screw were the same in both implant types. The diameter and length of the abutment screw that connectedthe implant and abutment measured 1.5 × 11 mm (Fig. 1d and e). The implants were vertically embedded in resins with 3 mm clearance from the platform to the resin. Abutments were tightened to 20 N cm by a torque gauge (BTG50CN, Tohnichi Mfg. Co. Ltd., Tokyo, Japan). Resins mimicked mechanical properties of cortical and cancellous bones (polyphenylene sulfide: 35 × 2 × 27 mm and polypropylene: 35 × 25 × 27 mm, Ensinger Japan, Tokyo, Japan, respectively) (Fig. 1f).

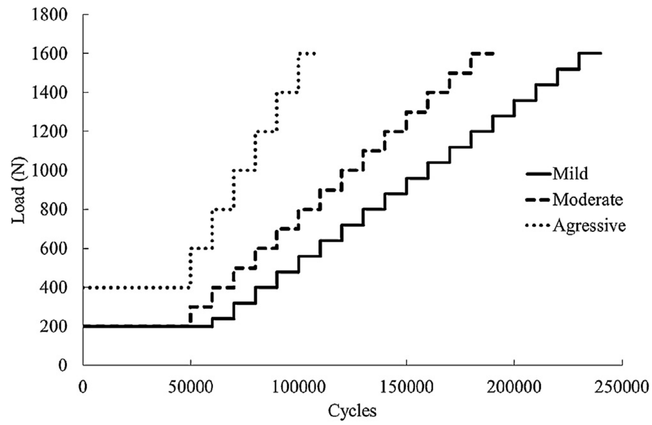

Fig. 2. SSALT profiles show the cycle-to-load assignment for specimens fatigued in the mild, moderate, or aggressive profile.

2.2. SSALT

SSALTs [19] were performed according to three fatigue profiles (mild: n = 3, moderate: n = 2, and aggressive: n = 1) (Fig. 2) using a servo-all-electric system (TestResources 800L, TestResources Inc., Shakopee, MN, USA) (Fig. 3a and b) at 2 Hz. For both implant groups, Weibull curves and reliabilities for completion of a mission at 1,000 N were obtained and mean loads to failure, scale parameter η, and shape parameter m were calculated. In addition, fatigue cracks were observed with a stereomicroscope (SMZ-745T, Nikon, Tokyo, Japan) using high dynamic range software (NIS-Elements Ver.4.0, Nikon, Tokyo, Japan). All specimens were analyzed by micro-CT (R_mCT2, Rigaku Corp., Tokyo, Japan) using a 59 μm image pixel size and classified according to fracture mode: intact abutment (Ia), fractured joint (Fj), fractured thread (Ft), fractured platform (Fp), fractured abutment screw (Fs), and bent abutment screw (Bs). The angles of crack lines occurring at Fp were measured by ImageJ software (public domain).

2.3. FEA

Using the same CAD models used for machining the SSALT fixtures and abutments, displacement vectors of implant components related to dislocation of a metallic crystal inducing fatigue crack initiation were analyzed by three-dimensional (3D) FEA (Solidworks2011, Dassault Systèmes Solidworks Corp, Waltham, MA, USA). Table 1 shows mechanical properties of each component used for 3D FEA. CAD models were standardized to make clear comparisons for only fixture-abutment joint types and excluded other multifactorial designs, such as diameter and length of the implant fixture. The implant fixture and abutment were connected by an abutment screw. The bottom and marginal surface of bone models were fixed and 20 N was loaded at the abutment at a 30-degree oblique angle to the long axis of the fixture (Fig. 3c). The angles between the implant fixture platforms and directions of the displacement vectors were measured corresponding to the Fp site using ImageJ software.

2.4. Statistical analysis

The angles obtained from *in vitro* SSALT and *in silico* 3D FEA were compared using two-way ANOVA (PASW Statistic 18, IBM, Somers, NY, USA). p values < 0.001 were considered statistically significant.

3. Results

Table 2 shows fracture modes of all specimens. Fractures were mainly observed at the top surface of the fixture platform (Fig. 4a and b) except for two specimens in IN and one specimen in EX. Fractures of two specimens in IN were observed at the second thread of the implant fixture (Fig. 4c); fractures in the specimen in EX and the other two specimens in IN were observed at the joint (Fig. 4d and e). In addition, abutment screws of three specimens in IN were fractured (Fig. 4e), while there was no fracture at the abutment or the abutment screw in EX.

Table 1
Mechanical properties for 3D FEA.

Component	Young's modulus (MPa)	Poisson's ratio
Cortical bone	14,000	0.30
Cancellous bone	1,470	0.30
Grade IV titanium	116,000	0.34

Mechanical properties were defined as previously described [21].

Weibull curves obtained from SSALT are presented in Fig. 5. The shape parameter m (two-sided at 90% confidence bounds) for EX and IN were 9.9 (4.1–14.2) and 7.8 (3.2–11.2), respectively; and the scale parameter η (two-sided at 90% confidence bounds) for EX and IN were 1212.9 (1103.2–1342.8) and 1431.7 (1268.8–1629.7) N, respectively. Greater reliability at 1,000 N, 1,200 N, and 1,400 N were recorded for IN (94.0%, 77.6%, and 43.2%) than EX (86.3%, 40.7%, and 1.6%).

Fatigue crack initiation was observed at the fractured platform of the implant fixture, and angles of crack lines of EX (*in vitro*: $137.6 \pm 4.5^{\circ}$) (Fig. 6a) were significantly greater than that of IN (*in vitro*: $114.8 \pm 4.3^{\circ}$) ($p < 0.001$) (Fig. 6b).

Fig. 7 shows the distribution of displacement vectors calculated by 3D FEA for EX and IN. The angles between the direction of the displacement vectors and the platform of the implant fixture for EX (*in silico*: $131.5 \pm 6.0^{\circ}$) (Fig. 7a), which corresponds to the location of the crack line *in vitro*, were significantly greater than that of IN (*in silico*: $117.1 \pm 1.8^{\circ}$) ($p < 0.001$) (Fig. 7b). In addition, the angles obtained from *in vitro* SSALT and *in silico* 3D FEA were not significantly different ($p = 0.324$), while those obtained in EX and IN showed a significant difference ($p < 0.001$) (Fig. 8).

4. Discussion

Previous studies of *in vitro* fatigue tests with commercially available implants suggested that implant fixtures with IN have greater fatigue resistance [11,12] and stability [14] and lower degrees of microgap [15] and bone loss [16] compared with those with EX. Conversely, some studies reported findings favoring fixtures with EX [25–27]. The discrepancy in results likely resulted from the multifactorial design of the implants evaluated, such as diameter and length of the implant fixture, fixture-abutment joints, and neck design of the fixtures. Therefore, the present study focused on the independent variable design and clarified that fixture-abutments with IN had greater fatigue resistance than those with EX *in vivo*.

Fractured platforms were observed in most specimens and there were no related studies detected in crack angles between fixtures with EX and those with IN. For fixtures with EX, a crack line was observed near the bottom edge of the hexagon structure, while that of fixtures with IN was observed near the buccal side of the screw hole in the fixture body. The edge and the screw hole, working as a small notch or a fixture defect, likely resulted in stress concentration associated with fatigue crack initiation [28].

Fractured joints were observed at the fixture of EX in one specimen and abutments of IN in two specimens, although most fractures occurred on the platform of the implant fixture in both implants with EX and IN. For EX, the boundary between the hexagonal structure and the platform has a mechanically weak configuration creating edge tensile forces. For IN, this boundary lies

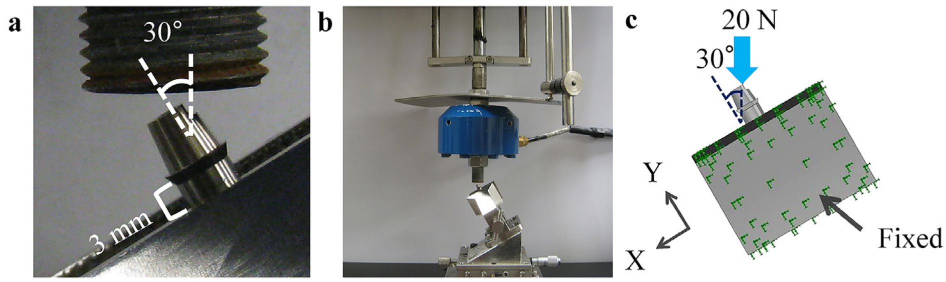

Fig. 3. Experimental setup of *in vitro* SSALTs and *in silico* 3D FEA. (a) Assembled implant embedded in a bone model. (b) Specimen for *in vitro* SSALT set on a servo-all-electric system. (c) Boundary conditions for *in silico* 3D FEA.

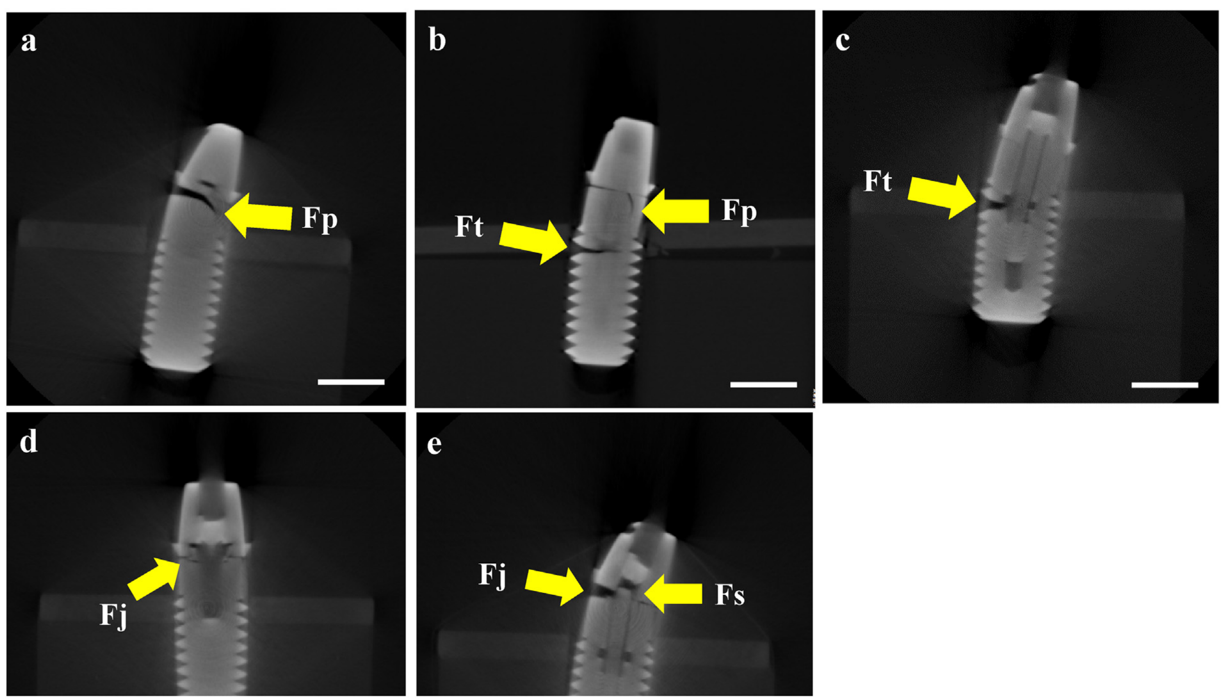

Fig. 4. Micro-CT images and fracture modes after *in vitro* SSALTs. Yellow arrows indicate fatigue fracture sites and scale bars indicate 10 mm. (a) Fractured platform (Fp). (b) Fp and fractured thread (Ft). (c) Ft. (d) Fractured joint (Fj). (e) Fj and fractured abutment screw (Fs).

Table 2
Fracture modes of specimens after SSALTs.

Specimen No.		1	2	3	4	5	6
External	Abutment	Ia	Ia	Ia	Ia	Ia	Ia
	Fixture	Fp	Fj	Fp	Fp	Fp	Fp
	Abutment screw	Bs	Bs	Bs	Bs	Bs	Bs
Internal	Abutment	Fj	Ia	Ia	Ia	Fj	Ia
	Fixture	Fp	Ft	Ft, Fp	Ft	Fp	Fp
	Abutment screw	Fs	Bs	Bs	Bs	Fs	Fs

Ia: intact abutment, Fj: fractured joint, Ft: fractured thread, Fp: fractured platform, Fs: fractured abutment screw, and Bs: bent abutment screw.

between the inner cylindrical part of the fixture and the bottom of the abutment.

A fractured abutment screw alone was observed in one specimen with EX, while a fractured joint was observed in addition to a fractured abutment screw in two specimens with IN. These observations suggest that fracturing of the abutment screw occurred before joint failure [13,29] because of its smaller diameter among the implant components, and this stress concentration was confirmed by *in silico* FEA [12]. Fractured threads with IN were observed associated with bent abutment screws. In clinical cases, complete removal of fractured implant fixture has been recommended as the best treatment option [30] though there are several clinical challenges [31]. These results suggest that fracture of abutment screws could prevent the

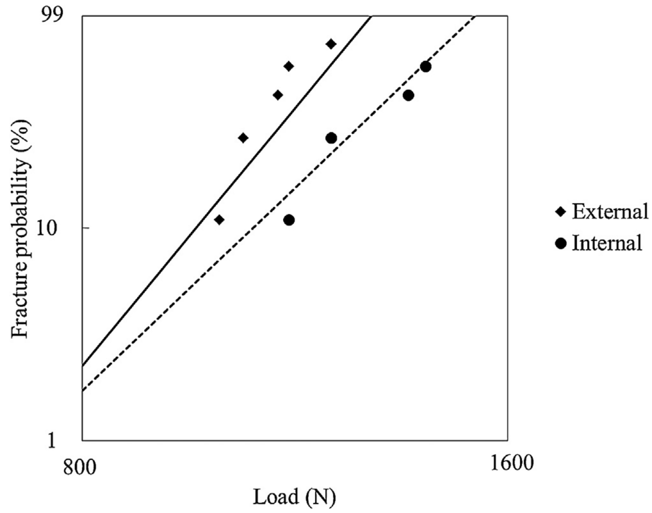

Fig. 5. Weibull curves from SSALTs using implants with external and internal joint types.

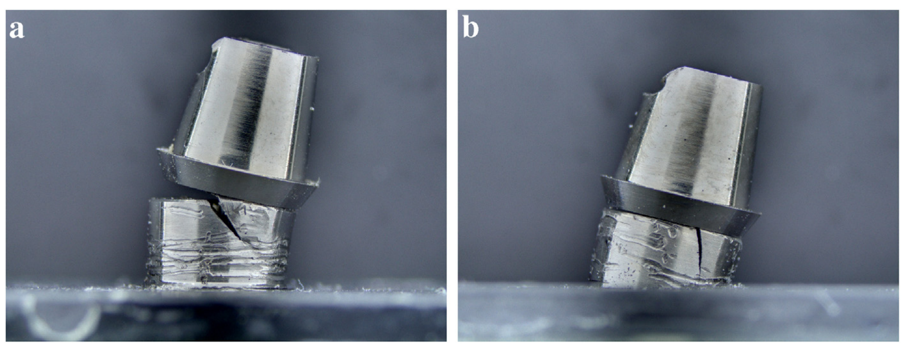

Fig. 6. Stereomicroscopic images processed by high dynamic range software. (a) Crack line at the platform with fractured joint of the external joint type. (b) Crack line at the platform with fractured abutment screw of the internal joint type.

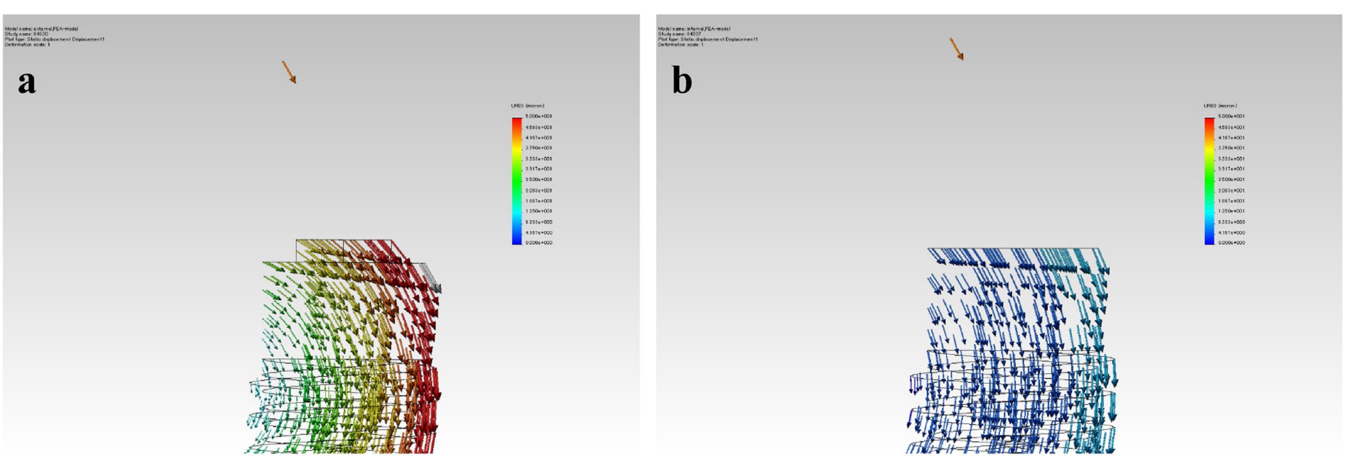

Fig. 7. Distribution of displacement vectors of the implant fixture obtained using *in silico* 3D FEA. (a) External joint type. (b) Internal joint type.

fractured thread, namely fracture of the implant fixture, in IN. Removal techniques of the fractured abutment screw have been reported in recent years [32–34].

In the Weibull analysis, the lower shape parameter m of implants with IN compared with implants with EX indicated greater variability in the strength which could be associated with various fracture modes (Table 2). In addition, the higher scale parameter η for IN indicated that the load in 63.2% of specimens that failed was higher than that of EX. Greater reliability for IN is consistent with results for commercial dental implants reported in other studies [11–13], even with mixed independent variables among studies.

The crack lines in implants with EX and IN observed *in vitro* were found to be along the direction of displacement vectors of the

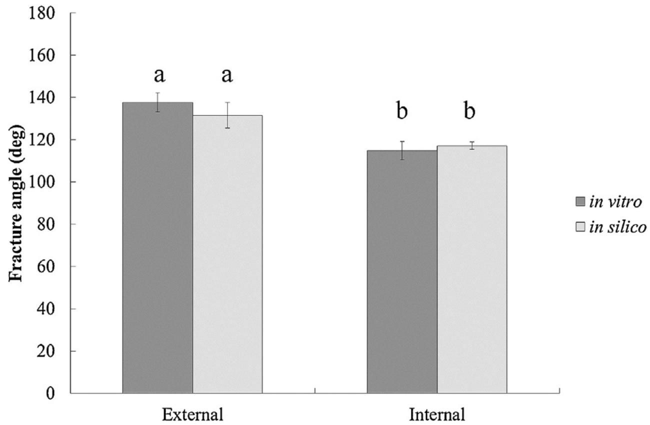

Fig. 8. Fractured angles *in vitro* and angles of displacement vectors of the platform surface *in silico* measured by ImageJ software. Values with different letter (a, b) designations are significantly different by two-way ANOVA ($p < 0.001$).

implant fixture by *in silico* 3D FEA. Our *in silico* findings suggest that displacement vectors have the potential to predict the direction of crack initiations in implants and may be helpful in device development for preventing fatigue crack propagation and implant failure in clinical cases [35]. Higher crack angles for IN than EX *in vitro* and *in silico* are consistent with the occurrence of vertical fractures along with marginal bone loss around fixtures with IN in clinical settings [35]. In addition, our results clarified that the design of the fixture-abutment joint type influenced the direction of vertical fracture. It is possible that one of the reasons for internal fixture vertical fracture [36] is shown by the direction of displacement vectors that occurred on the platform of the fixture.

Within the limitations of this study (few specimens and no prosthesis for either the *in vitro* fatigue testing or *in silico* 3D FEA), our results suggested that evaluation of the displacement *in silico* with static loading may predict the direction of crack initiation induced during *in vitro* SSALTs, which mimics long-term mouth motion in the oral cavity.

5. Conclusion

Our study demonstrated that *in silico* displacement vectors in the implant fixture would be helpful for development of new dental implant designs to map and reduce complex interactions leading to improved fatigue results *in vitro*.

Ethical approval

This article does not contain any studies with human participants or animals performed by any of the authors.

Informed consent

For this type of study, formal consent is not required.

Acknowledgment

This research was supported by a Grant-in-Aid for Scientific Research (No. JP15K11195) from the Japan Society for the Promotion of Science.

References

[1] Calvo-Guirado JL, Lopez-Lopez PJ, Perez-Albacete Martinez C, Javed F, Granero-Marin JM, Mate Sanchez de Val JE, et al. Peri-implant bone loss clinical and radiographic evaluation around rough neck and microthread implants: a 5-year study. Clin Oral Implant Res 2016, doi:http://dx.doi.org/10.1111/clr.12775.
[2] Dierens M, De Bruyn H, Kisch J, Nilner K, Cosyn J, Vandeweghe S. Prosthetic survival and complication rate of single implanttreatment in the periodontally healthy patient after 16 to 22 years of follow-up. Clin Implant Dent Relat Res 2016;18:117–28.
[3] Zembic A, Kim S, Zwahlen M, Kelly JR. Systematic review of the survival rate and incidence of biologic, technical, and esthetic complications of single implant abutments supporting fixed prostheses. Int J Oral Maxillofac Implants 2014;29(Suppl):99–116.
[4] Wang F, Zhang Z, Monje A, Huang W, Wu Y, Wang G. Intermediate long-term clinical performance of dental implants placed in sites with a previous early implant failure: a retrospective analysis. Clin Oral Implants Res 2015;26:1443–9.
[5] Rinke S, Roediger M, Eickholz P, Lange K, Ziebolz D. Technical and biological complications of single-molar implant restorations. Clin Oral Implants Res 2015;26:1024–30.
[6] Becker W, Goldstein M, Becker BE, Sennerby L. Minimally invasive flapless implant surgery: a prospective multicenter study. Clin Implant Dent Relat Res 2005;7(Suppl. 1):S21–7.
[7] Kim Y, Oh TJ, Misch CE, Wang HL. Occlusal considerations in implant therapy: clinical guidelines with biomechanical rationale. Clin Oral Implants Res 2005;16:26–35.
[8] Weng D, Nagata MJ, Bell M, Bosco AF, de Melo LG, Richter EJ. Influence of microgap location and configuration on the periimplant bone morphology in submerged implants. an experimental study in dogs. Clin Oral Implants Res 2008;19:1141–7.
[9] Weng D, Nagata MJ, Bosco AF, de Melo LG. Influence of microgap location and configuration on radiographic bone loss around submerged implants: an experimental study in dogs. Int J Oral Maxillofac Implants 2011;26:941–6.
[10] Abrahamsson I, Berglundh T, Lindhe J. The mucosal barrier following abutment dis/reconnection: an experimental study in dogs. J Clin Periodontol 1997;24:568–72.
[11] Almeida EO, Freitas Jr. AC, Bonfante EA, Marotta L, Silva NR, Coelho PG. Mechanical testing of implant-supported anterior crowns with different implant/abutment connections. Int J Oral Maxillofac Implants 2013;28:103–8.
[12] Freitas-Junior AC, Rocha EP, Bonfante EA, Almeida EO, Anchieta RB, Martini AP, et al. Biomechanical evaluation of internal and external hexagon platform switched implant-abutment connections: an in vitro laboratory and three-dimensional finite element analysis. Dent Mater 2012; 28:e218–28.
[13] Freitas Jr. AC, Bonfante EA, Rocha EP, Silva NR, Marotta L, Coelho PG. Effect of implant connection and restoration design (screwed vs: cemented) in reliability and failure modes of anterior crowns. Eur J Oral Sci 2011;119:323–30.
[14] Feitosa PC, de Lima AP, Silva-Concilio LR, Brandt WC, Neves AC. Stability of external and internal implant connections after a fatigue test. Eur J Dent 2013;7:267–71.
[15] Gil FJ, Herrero-Climent M, Lazaro P, Rios JV. Implant-abutment connections: influence of the design on the microgap and their fatigue and fracture behavior of dental implants. J Mater Sci: Mater M 2014;25:1825–30.
[16] Penarrocha-Diago MA, Flichy-Fernandez AJ, Alonso-Gonzalez R, Penarrocha-Oltra D, Balaguer-Martinez J, Penarrocha-Diago M. Influence of implant neck design and implant-abutment connection type on peri-implant health. Radiological study. Clin Oral Implants Res 2013;24:1192–200.
[17] Pozzi A, Agliardi E, Tallarico M, Barlattani A. Clinical and radiological outcomes of two implants with different prosthetic interfaces and neck configurations: randomized, controlled, split-mouth clinical trial. Clin Implant Dent Relat Res 2014;16:96–106.
[18] Coelho PG, Jimbo R. Osseointegration of metallic devices: current trends based on implant hardware design. Arch Biochem Biophys 2014;561:99–108.
[19] Bonfante EA, Coelho PG. A critical perspective on mechanical testing of implants and prostheses. Adv Dent Res 2016; 28:18–27.
[20] Yamanishi Y, Yamaguchi S, Imazato S, Nakano T, Yatani H. Influences of implant neck design and implant-abutment joint type on peri-implant bone stress and abutment micromovement: three-dimensional finite element analysis. Dent Mater 2012;28:1126–33.
[21] Yamanishi Y, Yamaguchi S, Imazato S, Nakano T, Yatani H. Effects of the implant design on peri-implant bone stress and abutment micromovement: three-dimensional finite element analysis of original computer-aided design models. J Periodontol 2014;85:e333–8.
[22] Toniollo MB, Macedo AP, Rodrigues RC, Ribeiro RF, Mattos Mda G. Three-dimensional finite element analysis of the stress distribution on morse taper implants surface. J Prosthodont Res 2013;57:206–12.
[23] Tang CB, Liul SY, Zhou GX, Yu JH, Zhang GD, Bao YD, et al. Nonlinear finite element analysis of three implant-abutment interface designs. Int J Oral Sci 2012;4:101–8.
[24] Tabata LF, Rocha EP, Barao VA, Assuncao WG. Platform switching: biomechanical evaluation using three-dimensional finite element analysis. Int J Oral Maxillofac Implants 2011;26:482–91.
[25] Machado LS, Bonfante EA, Anchieta RB, Yamaguchi S, Coelho PG. Implant-abutment connection designs for anterior crowns: reliability and failure modes. Implant Dent 2013;22:540–5.
[26] Ribeiro CG, Maia MLC, Scherrer SS, Cardoso AC, Wiskott HWA. Resistance of three implant-abutment interfaces to fatigue testing. J App Oral Sci 2011;19:413–20.

[27] Tsuge T, Hagiwara Y, Matsumura H. Marginal fit and microgaps of implant-abutment interface with internal anti-rotation configuration. Dent Mater J 2008;27:29–34.

[28] Mitchell MR, Smith SW, Woods T, Berg B. ASTM international. fatigue and fracture of medical metallic materials and devices. West Conshohocken, PA: ASTM International; 2014 p. vii, 163 pp.

[29] Khraisat A, Stegaroiu R, Nomura S, Miyakawa O. Fatigue resistance of two implant/abutment joint designs. J Prosthet Dent 2002;88:604–10.

[30] Marcelo CG, Filie Haddad M, Gennari Filho H, Marcelo Ribeiro Villa L, Dos Santos DM, Aldieris AP. Dental implant fractures—aetiology, treatment and case report. J Clin Diagn Res 2014;8:300–4.

[31] Muroff FI. Removal and replacement of a fractured dental implant: case report. Implant Dent 2003;12:206–10.

[32] Yoon JH, Lee H, Kim MY. Safe removal of a broken abutment screw with customized drill guide and rotary snstrument: a clinical report. J Prosthodont 2016;25:170–3.

[33] Imam AY, Moshaverinia A, Chee WW, McGlumphy EA. A technique for retrieving fractured implant screws. J Prosthet Dent 2014;111:81–3.

[34] Walia MS, Arora S, Luthra R, Walia PK. Removal of fractured dental implant screw using a new technique: a case report. J Oral Implantol 2012;38:747–50.

[35] Jimbo R, Halldin A, Janda M, Wennerberg A, Vandeweghe S. Vertical fracture and marginal bone loss of internal-connection implants: a finite element analysis. Int J Oral Maxillofac Implants 2013;28:e171–6.

[36] Takeshita K, Toia M, Jinno Y, Sumi T, Takahashi T, Halldin A, et al. Implant Vertical Fractures Provoked by Laboratory Procedures: A Finite Element Analysis Inspired from Clinical Cases. Implant Dent 2016;25:361–6.